Spectral Properties of Fluorescent Derivatives of the Oligomycin Sensitivity Conferring Protein and Analysis of Their Interaction with the F_1 and F_o Sectors of the Mitochondrial ATPase Complex†

Jerzy Duszynski,‡ Alain Dupuis,*,§ Béatrice Lux,‖ and Pierre V. Vignais§

Department of Cellular Biochemistry, Nencki Institute of Experimental Biology, 3 Pasteur Street, 02-093 Warsaw, Poland, Laboratoire de Biochimie (UA CNRS 1130), Département de Recherche Fondamentale, Centre d'Etudes Nucléaires, 85X, 38041 Grenoble Cedex, France, and Laboratoire de Physique de la Faculté de Pharmacie (UA CNRS 491), Université Louis Pasteur, BP 10, 67048 Strasbourg Cedex, France

Received November 5, 1987; Revised Manuscript Received April 21, 1988

ABSTRACT: In order to study the kinetics and the nature of the interactions between the oligomycin sensitivity conferring protein (OSCP) and the F_o and F_1 sectors of the mitochondrial ATPase complex, fluorescent derivatives of OSCP, which are fully biologically active, have been prepared by reaction of OSCP with the following fluorescent thiol reagents: 6-acryloyl-2-(dimethylamino)naphthalene (acrylodan), 2-(4-maleimidylanilino)naphthalene-6-sulfonic acid (Mal-ANS), *N*-(1-pyrenyl)maleimide (Mal-pyrene), 7-(diethylamino)-3-(4-maleimidylphenyl)-4-methylcoumarin (Mal-coumarin), and fluorescein 5-maleimide (Mal-fluorescein). The preparation of these derivatives was based on the previous finding that the single cysteinyl residue of OSCP, Cys 118, can be covalently modified by alkylating reagents without loss of biological activity [Dupuis, A., Issartel, J. P., Lunardi, J., Satre, M., & Vignais, P. V. (1985) *Biochemistry 24*, 728–733]. For all fluorescent probes used, except Mal-pyrene and Mal-fluorescein, the emission spectra of conjugated OSCP were blue-shifted relative to those of the corresponding mercaptoethanol adducts, indicating that the fluorophores attached to Cys 118 were located in a hydrophobic pocket. These results were consistent with the high quantum yields and the increased fluorescence lifetimes of conjugated OSCP compared to mercaptoethanol adducts in aqueous buffer. They also fit with quenching data obtained with potassium iodide which showed that the fluorophore is shielded from the aqueous medium when it is attached to Cys 118 of OSCP. Especially noticeable was the wide half-width of the OSCP–acrylodan emission peak compared to that of mercaptoethanol–acrylodan. Denaturation of OSCP conjugated to Mal-ANS or acrylodan resulted in a red shift of the emission spectrum; in other words, the Cys 118 environment which was sequestered in a hydrophobic pocket in native OSCP became exposed to the aqueous medium in denatured OSCP. Binding of F_1 to OSCP fluorescent derivatives led to the following modifications of the fluorescence parameters: (1) a red shift of the emission peak of OSCP–acrylodan and OSCP–Mal-ANS, (2) a narrowing of the emission peak of OSCP–acrylodan, (3) a decrease of the lifetime of OSCP–Mal-pyrene, and (4) a decrease of the quantum yield of OSCP–Mal-coumarin, OSCP–Mal-pyrene, and OSCP–Mal-ANS. These modifications were interpreted by exposure of Cys 118 to a more hydrophilic environment when OSCP binds to F_1. Polarization assays carried out with OSCP–Mal-pyrene in both the absence and presence of F_1 pointed to the existence of some rotational freedom of OSCP–Mal-pyrene bound to F_1. The fast fluorescence changes reflecting the reaction of OSCP–acrylodan with F_1 (less than 1 s at 25 °C) contrasted the slow fluorescence changes (several minutes) occurring upon binding of OSCP–acrylodan or F_1–OSCP–acrylodan to F_o in AUA particles (submitochondrial particles depleted of F_1 and OSCP). The Cys 118 residue of OSCP–acrylodan, which had become exposed to the aqueous medium upon binding of F_1, was shielded again upon addition of AUA particles, as a result of the formation of an F_o–F_1–OSCP complex.

ATP synthesis is catalyzed by the mitochondrial F_1–F_o complex at the expense of the proton motive force generated by the mitochondrial respiratory chain. Two mechanisms have been advanced to explain how the proton flux through the F_o sector is used to drive ATP synthesis at the level of the F_1 sector: (1) a direct mechanism in which protons are involved in condensation of ADP and P_i at the catalytic site; (2) an indirect mechanism in which the proton motive force is used to induce conformational changes in F_1 [for review, see Nicholls (1982)]. Understanding interactions between the two sectors of the F_1–F_o complex may provide new insight into the mechanism of ATP synthesis. During the last few years, we have been interested in a small peptide, the oligomycin sensitivity conferring protein (OSCP)[1] ($M_r \simeq 21\,000$), which in-

† This work was supported by grants from the Centre National de la Recherche Scientifique (CNRS/UA 1130), the Institut de la Santé et de la Recherche Médicale, and the Université Joseph Fourier, Faculté de Médecine, Grenoble.

* Address correspondence to this author at the DRF/Biochimie, C.E.N.-G., 85X, 38041 Grenoble Cedex, France.

‡ Nencki Institute of Experimental Biology.

§ Centre d'Etudes Nucléaires.

‖ Université Louis Pasteur.

[1] Abbreviations: DTNB, 5,5′-dithiobis(nitrobenzoate); NEM, *N*-ethylmaleimide; acrylodan, 6-acryloyl-2-(dimethylamino)naphthalene; Mal-ANS, 2-(4-maleimidylanilino)naphthalene-6-sulfonic acid; Mal-pyrene, *N*-(1-pyrenyl)maleimide; Mal-coumarin, 7-(diethylamino)-3-(4-maleimidylphenyl)-4-methylcoumarin; Mal-fluorescein, fluorescein 5-maleimide; OSCP, oligomycin sensitivity conferring protein; F_1, catalytic sector of mitochondrial ATPase; F_o, proton channel of mitochondrial ATPase; TPCK, *N*-tosyl-L-phenylalanine chloromethyl ketone; AUA particles, submitochondrial particles depleted of F_1 and OSCP.

0006-2960/88/0427-6288$01.50/0

teracts with both F_1 and F_o of the mitochondrial ATPase complex. The biological activity of OSCP can be readily assayed by its ability to make the catalytic sector, F_1, of the ATPase complex sensitive to inhibition by oligomycin, an antibiotic that binds to F_o. Although it is clear that OSCP controls interactions between the F_1 and F_o sectors of this complex, the mechanism by which these interactions are controlled is still enigmatic and a number of questions remain to be answered. For example, does OSCP actually act as the link between the F_1 and F_o sectors? Is it involved in channeling protons from the F_o sector to the F_1 sector of the ATPase channel? Does it control only the F_o–F_1 interaction by modifying the conformation of F_1 in such a way that F_1 binds more tightly, but directly to F_o?

The amino acid sequence of OSCP (Ovchinnikov et al., 1984) shows the presence of a single cysteinyl residue, Cys 118, located in the middle of the peptide chain. Modification of OSCP by covalent reaction with thiol reagents has been used in previous studies to obtain radiolabeled and photoactivable derivatives of OSCP (Dupuis et al., 1985a; Dupuis & Vignais, 1985). These derivatives were as active in conferring oligomycin sensitivity to F_1 as native OSCP. In other words, they were able to recognize and react with the same components of the ATPase complex as native OSCP and were therefore useful for studying the topographical relationship of OSCP with the F_1 and F_o sectors of the ATPase complex. On the other hand, kinetic studies of OSCP interactions required optical methods. For this purpose, the panoply of OSCP derivatives was recently augmented by a fluorescent derivative prepared by conjugation of acrylodan (Prendergast et al., 1983) to OSCP (Dupuis et al., 1987). We have extended this preliminary study on acrylodan–OSCP to a number of fluorescent derivatives of OSCP prepared by reaction of fluorescent thiol reagents with the Cys 118 residue of OSCP. We report here the spectral properties of these fluorescent OSCP derivatives. The polar, nonpolar environment of Cys 118 in OSCP and its accessibility have been assessed from emission spectra, fluorescence lifetimes, and quenching by potassium iodide. The same approaches have been used to monitor modifications of the environment and accessibility of Cys 118 upon binding of fluorescent OSCP to F_1 and/or F_o.

Materials and Methods

Biological Preparations. Mitochondria were prepared according to Smith (1967). F_1 and OSCP were purified as described by Knowles and Penefsky (1972) and by Senior (1979), respectively. F_1- and OSCP-depleted submitochondrial particles (AUA particles) were prepared as described previously (Dupuis & Vignais, 1987), with omission of the last step of sonication during OSCP extraction as suggested by others (Penin et al., 1986; Ernster et al., 1986). Proteins were measured by the Coomassie blue binding method (Bradford, 1936) for soluble proteins and by the method of Folin for membrane proteins (Zak & Cohen, 1961). The oligomycin sensitivity of ATPase in the F_1–F_o complex reconstituted in the presence of OSCP was measured as reported previously (Dupuis et al., 1983a).

OSCP Labeling. The fluorescent sulfhydryl reagents used in the present work were purchased from Molecular Probes (Eugene, OR). They were dissolved to a concentration of approximately 40 mM in the appropriate solvent and used within 48 h of preparation. The solvents used for the different reagents were as follows: acetonitrile for acrylodan and Mal-coumarin; dimethylformamide for Mal-fluorescein and Mal-pyrene; aqueous buffer for Mal-ANS. OSCP (100 μM) previously dialyzed against 0.1 M phosphate buffer, pH 7.0, was incubated with a 5-fold excess of fluorescent probes (500 μM) for 15 h at 4 °C in the dark. Unreacted probe was separated from OSCP-bound probe by filtration–centrifugation through a G-50 column equilibrated in 20 mM Hepes buffer and 100 mM KCl, pH 7.4.

Spectral Measurements. Fluorescence spectra were recorded on a SLM 8000 fluorometer equipped with a thermostated cuvette holder and a magnetic stirring device with correction for source and photomultiplier variations. All experiments were carried out at 25 °C in a standard medium consisting of 20 mM Hepes, 100 M KCl, and 0.02% Tween 20, pH 7.4. The background due to the solvent and the dark current was deducted from each spectrum. Corrected fluorescence emission spectra were used to obtain fluorescence quantum yields relative to that of quinine sulfate (Parker & Rees, 1960). The reference value for the quantum yield of quinine sulfate was 0.53 (Adams et al., 1977).

Lifetime measurements were performed with a laboratory-flash photon-counting apparatus (Gérard et al. 1972). The fluorescence decay profiles were analyzed statistically by using the residual distribution form (Grinwald & Steinberg, 1974; Grinwald, 1976). For quenching studies, increasing amounts of a 4 M KI and 100 μM $Na_2S_2O_3$ solution, pH 7.5, were added to the OSCP fluorescent adduct. A control experiment was run in parallel with KCl substituted to KI. The fluorescence intensities in the absence of the quencher (F_0) and its presence (F) were corrected for dilution and ionic strength, by using values obtained in the presence of KCl. Experimental data were analyzed by the Stern–Volmer equation:

$$F_0/F = 1 + K[Q] = 1 + k_q\tau_0[Q] \quad (1)$$

where [Q] is the quencher concentration and K is the Stern–Volmer constant, i.e., the product of the kinetic constant k_q of the quenching process and the mean lifetime τ_0 of the fluorophore attached to the protein in the absence of quencher.

Polarization assays were carried out by using three Glan–Thomson calcite prism polarizers with the SLM 8000 fluorometer in the T configuration. Parallel and perpendicular polarized light beams were passed through filters with an appropriate wavelength cutoff. The polarization (P) was derived from the equation:

$$P = (F_{VV} - GF_{VH})/(F_{VV} + GF_{VH}) \quad (2)$$

where F_{VV} and F_{VH} correspond to the measured fluorescence intensities for parallel and perpendicular polarization of the emitted light, respectively, and the correction factor G is the ratio of the sensitivites of the detection system for vertically and horizontally polarized light. Factor G was obtained with the excitation polarizer in the horizontal position (90°). The relaxation time ρ was deduced from the fluorescence polarization values by using an alternative form of the Perrin equation:

$$\left(\frac{1}{P} - \frac{1}{3}\right) = \left(\frac{1}{P_0} - \frac{1}{3}\right)\left(1 + \frac{3\tau}{\rho}\right) \quad (3)$$

where ρ is the rotational relaxation rate of the molecule carrying the fluorescent probe, τ is the fluorescence lifetime, P is the measured polarization, and P_0 is the extrapolated value of P at infinite viscosity. The relaxation time ρ for a spherical protein can be calculated from the relation:

$$\rho = \frac{3\eta V}{kT} \quad (4)$$

where η is the medium viscosity, k is Boltzmann's constant,

T is the absolute temperature, and V is the volume of the spherical protein.

The equation used for plots of polarization as a function of the viscosity of the medium was obtained by substituting eq 4 into eq 3, which yields

$$\left(\frac{1}{P} - \frac{1}{3}\right) = \left(\frac{1}{P_0} - \frac{1}{3}\right)\left(1 + \frac{RT\tau}{\eta V}\right)$$

The intercept of the plots of $1/P$ vs T/η is $1/P_0$, i.e., the reciprocal of polarization at infinite viscosity.

Absorption spectra were recorded with a Cary 219 spectrophotometer. The labeling stoichiometries for the fluorescent thiol reagents used in this study were determined on the basis of the absorption coefficients reported in literature for the corresponding thiol adducts in aqueous medium (cf. Table I), except for the acrylodan–mercaptoethanol adduct, which we determined directly. Free probes and thiol adducts were analyzed by thin-layer chromatography on silica plates (Whatman K6), with either ether/acetic acid (98/2 v/v) or 0.15 M sodium citrate/butanol/ethanol (1/1/10 v/v/v) as solvent, and visualized under UV light. Fluorescence of the free probes was enhanced by spraying with mercaptoethanol. To localize fluorescent labels in the amino acid sequence of OSCP, the labeled OSCP was fragmented into short peptides, which were resolved by HPLC, and analyzed for bound fluorescence. First, the modified OSCP was extensively dialyzed against 0.1 M ammonium bicarbonate, pH 7.8, and then digested with TPCK–trypsin (Worthington) for 18 h at 30 °C with a trypsin to OSCP ratio of 1/40 (w/w). The resulting hydrolysate was analyzed by HPLC (Waters) using a Brownlee C8 column to which an acetonitrile gradient in 10 mM trifluoroacetic acid was applied. Elution of peptides was monitored by absorbance at 215 nm. Fluorescence was measured with a Waters 420 fluorescence detector.

Results

Labeling Stoichiometry of OSCP with Thiol Fluorescent Reagents. The reactivity toward OSCP of the fluorescent thiol reagents acrylodan, Mal-ANS, Mal-pyrene, Mal-fluorescein, and Mal-coumarin was examined. With all probes except Mal-fluorescein, the fluorescence intensity was increased upon addition of OSCP, indicating reaction with the protein. A preliminary titration assay was carried out (not shown), which consisted in measuring the increase of the fluorescence intensity with respect to the concentration of the added probe and the length of the incubation period, as described for the titration of Na^+/K^+-ATPase by Mal-ANS (Gupte & Lane, 1979). The standard conditions for saturation derived from this titration, namely, a 15-h incubation at 4 °C, with 500 μM fluorescent probe and 100 μM OSCP, were used to determine binding stoichiometries. Following incubation of a given fluorescent probe with OSCP, the conjugated OSCP was separated by centrifugation–filtration on Sephadex G-50 (cf. Materials and Methods), and its absorbance in the eluate was measured, using extinction coefficients reported in literature. The molar ratio of bound fluorescent probe to OSCP ranged from 0.66 to 1.25, except for OSCP–acrylodan, for which this ratio amounted to 1.5–1.7 (Table I). If the probes bind specifically to the single cysteinyl residue of OSCP, this molar ratio would be expected to be 1, or close to 1. Deviation from this value reflects either an erroneous quantification of the bound probe, or labeling of residues other than Cys 118 in the OSCP molecule. With respect to the first hypothesis, it should be noted that calculation of the amount of bound probe in the OSCP adducts was based on the extinction coefficients of the corresponding mercaptoethanol adducts in water. The possibility cannot, of course, be excluded that the absorbance of a given probe bound to OSCP is different from that of the same probe bound to mercaptoethanol. In fact, the spectral properties of a bound probe are likely to be sensitive to the polarity of its environment. For example, the absorption coefficient of free acrylodan increases from 12990 M^{-1} to 16400 M^{-1}, and the emission peak is shifted from 360 to 387 nm, when water is replaced by ethanol as solvent (Prendergast et al., 1983). Likewise, the extinction coefficient of Mal-ANS in water is increased by 14% when Mal-ANS combines with mercaptoethanol and is further increased by 25% when water is replaced by ethanol (personal data). It is therefore presumed that the polarity of the environment of the probe bound to OSCP directly influences the fluorescent properties of this probe.

Table I: Labeling Stoichiometry of OSCP by Different Fluorescent Thiol Probes. Protection Afforded by NEM against Binding of Fluorescent Probes

probe	wavelength (nm)	absorption coefficient (M^{-1} cm^{-1})	ref	probe/OSCP ratio (mol/mol)
acrylodan	360	16 500	this work	1.5–1.7 (2)[a]
Mal-ANS	322	20 000	Gupte and Lane (1983)	1.25 ± 0.25 (3)
Mal-fluorescein	490	70 800	Richter et al. (1985)	1.02 ± 0.06 (3)
Mal-pyrene	343	37 500	Richter et al. (1985)	0.85 ± 0.16 (3)
Mal-coumarin	387	30 200	Richter et al. (1985)	0.66 ± 0.18 (3)

[a] Number of determinations. OSCP adducts were dissolved in standard medium (cf. Materials and Methods).

With regard to the second explanation for the deviation of the value of 1 for the molar ratio of bound probe to OSCP, namely, that the probe binds to several amino acid residues in OSCP, Lux and Gérard (1981) discussed the possibility that the applicability of Mal-pyrene to the analysis of protein structure has limitations linked to the unspecific (possibly noncovalent) binding of this probe. To rule out noncovalent attachment of the probes, the OSCP-bound probes recovered by gel filtration chromatography were subjected to thin-layer chromatography on silica gel (cf. Materials and Methods). No significant traces of fluorescence was detected at the level of the expected migration of the free probes, indicating that the probes were covalently attached to OSCP.

To ascertain that the fluorescent thiol probes used bound only to one amino acid residue in OSCP, i.e., the cysteinyl residue, Cys 118, the modified OSCP was subjected to tryptic digestion and the resulting peptides in the digest were analyzed by HPLC, as described under Materials and Methods. DTNB was used as a control, since this reagent, which is highly specific for thiol groups, is expected to react only with Cys 118 in OSCP. The elution patterns of the tryptic digest of OSCP modified by DTNB, monitored spectrophotometrically at 215 nm, differed from that of native OSCP by the disappearance of the peak eluted at 50 min and the appearance of a new peak eluted at 47 min (Figure 1A). The peptide fragment containing Cys 118 therefore corresponds to the 50-min peak and is recovered in the 47-min peak after DTNB modification. The same trypsin treatment was applied to OSCP modified by Mal-coumarin, Mal-pyrene, acrylodan, and

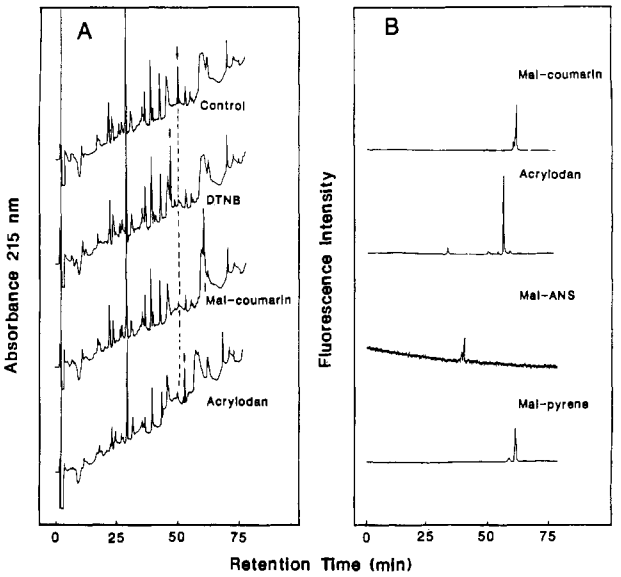

FIGURE 1: HPLC analysis of a tryptic digest of native OSCP and fluorescent derivatives of OSCP. Native and modified OSCP were digested with trypsin for 18 h at 30 °C in 0.1 M ammonium bicarbonate, pH 7.8, using a trypsin to OSCP ratio of 1/40 (w/w). An aliquot corresponding to about 1 nmol of digested OSCP was injected in a Brownlee C8 reverse-phase column equilibrated in 10 mM TFA and 5% acetonitrile. A linear gradient of acetonitrile was applied to reach a concentration of 75%. (A) Photometric monitoring of peptide fragments at 215 nm. The figure shows the profiles of elution of trypsin digests concerning (1) unmodified OSCP, (2) DTNB-modified OSCP containing 0.95 nmol of TNB/mol of OSCP, (3) OSCP–Mal-coumarin containing 0.74 mol of coumarin/mol of OSCP, and (4) OSCP–acrylodan containing 1.4 mol of acrylodan/mol of OSCP (labeling ratio estimated spectrophotometrically; cf. Table I). Among the numerous peptides generated from digested OSCP, only that one which was eluted at 50 min for native OSCP was absent in all modified OSCP. The lacking peptide was replaced by another one eluted at 47 min for OSCP–TNB, at 60 min for OSCP–Mal-coumarin, and at 55 min for OSCP–acrylodan (indicated by arrows). (B) Fluorometric monitoring of labeled peptides. Elution was followed by monitoring fluorescence with a Waters 420 detector [excitation filter 340 ± 6 nm; emission filter 425 nm (long pass)]. For Mal-pyrene, a 395-nm emission filter (long pass) was used. The Figure shows the elution of fluorescent peptides present in hydrolysates of (1) OSCP–Mal-coumarin, (2) OSCP–acrylodan, (3) OSCP–Mal-ANS, and (4) OSCP–Mal-pyrene.

Mal-ANS; in all cases, the 50-min peak disappeared, and new peaks appeared, which were characterized by retention times of 60 min for digests of OSCP–Mal-coumarin and OSCP–Mal-pyrene and 55 and 40 min for digests of OSCP–acrylodan and OSCP–Mal-ANS, respectively. By monitoring fluorometrically the elution of the tryptic digest of labeled OSCP, a major peak was found, which corresponded to more than 85% of the eluted fluorescence, accompanied by a few minor ones in the case of OSCP–Mal-coumarin, OSCP–Mal-pyrene, and OSCP–acrylodan (Figure 1B). In the case of OSCP–Mal-ANS, the satellite peak adjacent to the major one represented 30% of the total bound fluorescence. The question arose as to whether the peptides present in the small fluorescent peaks were different from that present in the major peak, thereby reflecting different localizations of the fluorescent probe on OSCP, or if they were derived from the major fluorescent peptide by further degradation. However, even in the first case, the level of contamination was clearly too low (except for OSCP–Mal-ANS) to be considered a serious drawback. In summary, from the analysis of a tryptic digest of fluorescent derivatives of OSCP, it can be safely concluded (with some reservations for OSCP–Mal-ANS) that the different probes used bind specifically at the only cysteinyl residue of OSCP, i.e., Cys 118. It is noteworthy that the pH used for modification of OSCP by the fluorescent thiol reagents was 7.0. At pH values higher than 7.5, nonspecific covalent binding probably occurs at amino acid residues other than Cys 118.

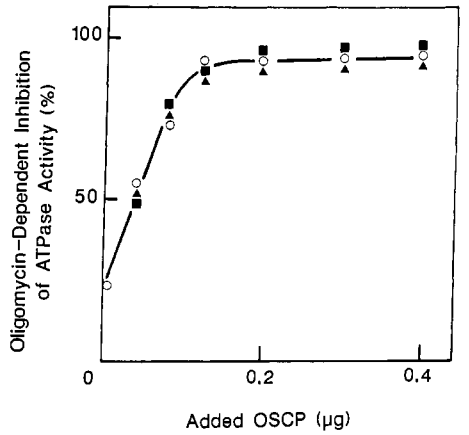

FIGURE 2: Ability of fluorescent derivatives of OSCP to confer oligomycin sensitivity of F_1-ATPase in a reconstituted F_1–F_o system. AUA particles (0.13 mg of protein) were preincubated at 30 °C for 10 min with 1.5 μg of F_1 and increasing amounts of OSCP as indicated in the figure in 0.45 mL of standard medium (cf. Materials and Methods). Then ATPase activity of aliquot fractions was measured in an ATP-regenerating system as described by Dupuis et al. (1983). Native OSCP (○), OSCP–acrylodan (▲), OSCP–Mal-ANS (■). In a similar assay (not shown), native OSCP, OSCP–Mal-fluorescein, OSCP–Mal-coumarin, and OSCP–Mal-pyrene exhibited the same biological activities.

Table II: Effect of Solvent Polarity on Maximum Emission of Fluorescent Probes

	relative blue shift of emission, $\Delta\bar{\nu}$ (cm^{-1})[b]		
probe[a]	mercaptoethanol adduct in ethanol	mercapto-ethanol adduct in aceto-nitrile	OSCP adduct in standard medium
acrylodan	1470	2740	2380
Mal-ANS	2340	2400	1220
Mal-coumarin	520	520	430
Mal-pyrene	0	0	0

[a] Unexpectedly, the emission of mercaptoethanol–Mal-fluorescein in ethanol (not shown) was red-shifted with respect to the emission of the same adduct in standard medium ($\Delta\bar{\nu}$) = 300 cm^{-1}). The emission of OSCP–Mal-fluorescein in standard medium was also red-shifted compared to that of mercaptoethanol–Mal-fluorescein in standard medium ($\Delta\bar{\nu}$ = −70 cm^{-1}). [b] Blue shift (expressed in terms of wavenumber in cm^{-1}) is related to emission of the mercaptoethanol adduct in standard medium.

All fluorescent OSCP derivatives were checked for their ability to confer oligomycin sensitivity to F_1-ATPase in a reconstituted F_1–F_o system and were found to be as efficient as native OSCP (Figure 2).

Spectral Properties of OSCP–Fluorescent Probe Adducts. In Tables II and III are compiled spectral properties relative to the adducts formed by reaction of OSCP with acrylodan, Mal-ANS, Mal-pyrene, Mal-fluorescein, and Mal-coumarin and, for comparison, those of the corresponding fluorescent adducts with mercaptoethanol. Due to their chemical structure, these different probes exhibited specific responses to changes in their environment. For example, the emission spectra of acrylodan, Mal-ANS, and Mal-coumarin conjugates were far more sensitive to solvent polarity than those of Mal-fluorescein and Mal-pyrene conjugates, as shown by the blue shift of their emission maxima (Table II). Consequently, acrylodan, Mal-ANS, and Mal-coumarin may be considered as appropriate tools to assess the polarity of the site to which they are bound. Yet probe–solvent interactions are a potential

Table III: Spectral Properties of Fluorescent OSCP and Mercaptoethanol Derivatives. Effect of Isolated F_1 on the Spectral Properties of Fluorescent OSCP Derivatives[a]

adduct	ex λ_{max} (nm)	em λ_{max} (nm)	Q^b	τ^c (ns)
OSCP–acrylodan	385	480	0.20	3.9
OSCP–acrylodan + F_1	385	495	0.21	3.8
mercaptoethanol–acrylodan	385	542	0.18	2.0
OSCP–Mal-ANS	323	422	0.16	8.0[d]
OSCP–Mal-ANS + F_1	323	429	0.11	7.7[d]
mercaptoethanol–Mal-ANS	323	445	0.02	2.0
OSCP–Mal-coumarin	387	475	0.68	3.6
OSCP–Mal-coumarin + F_1	387	475	0.56	3.6
mercaptoethanol–Mal-coumarin	387	485	0.28	2.3
OSCP–Mal-pyrene	345	376	0.32	88
OSCP–mal-pyrene + F_1	345	376	0.24	72
mercaptoethanol–Mal-pyrene	345	376	0.04	5.9
OSCP–Mal-fluorescein	495	522	0.62	4.1
OSCP–Mal-fluorescein + F_1	495	522	0.60	4.1
mercaptoethanol–Mal-fluorescein	495	520	0.53	3.9

[a] The medium used was standard medium. [b] Quantum yield. [c] Fluorescence lifetime. [d] The τ value given for OSCP–Mal-ANS is a mean value due to heterogeneity. Actually, the experimental data could be fitted to a biexponentional decay curve with the following lifetimes and relative populations of emitting molecules: OSCP–Mal-ANS, τ_1 5.5 ns (27%) and τ_2 9.0 ns (73%); OSCP–Mal-ANS + F_1, τ_1 1.9 ns (6%) and τ_2 8.1 ns (94%). For the other adducts, the time course of fluorescence decay was fitted to a single exponential curve.

source of artifacts. This is illustrated by the acrylodan–mercaptoethanol adduct, which exhibits a shift of its emission maximum quite different in the presence of ethanol and acetonitrile (Table II), despite the fact that the two solvents have the same polarizability index, equal to 0.3 (Weber & Farris, 1979). With these few examples, it is clear that pitfalls caused by the specific chemical nature of a given fluorescent probe can be avoided with the use of several related probes, as was the case in the present study.

The blue shift of the peak of maximum emission observed for adducts of OSCP with acrylodan, Mal-coumarin, and Mal-ANS compared to the adducts of mercaptoethanol with the same probes (Table III) indicates that these probes bound to OSCP experienced in the surrounding of Cys 118 a hydrophobic environment comparable to acetonitrile or ethanol (Table II). The apparent lower hydrophobicity observed with Mal-ANS might be explained by the contribution of Mal-ANS molecules unspecifically bound (see above) to peripheral reactive amino acid residues in OSCP such as lysine residues or may be due to the relative hydrophilic nature of the ANS moiety of Mal-ANS which should favor the extrusion of ANS from the hydrophobic pocket surrounding Cys 118 in OSCP. The conclusion that the probes bound to OSCP were not directly exposed to the aqueous medium was corroborated by the finding that the quantum yield and the lifetimes were higher for the OSCP conjugates than for the mercaptoethanol adducts in aqueous medium (Table III). This holds true, particularly for Mal-pyrene which showed an 8-fold increase in its quantum yield and a 15-fold increase in its lifetime, when bound to OSCP.

The half-width of the fluorescence emission peak is a complex function that depends in particular on the relaxation of the solvent molecules around the probe in its excited state. In the case of acrylodan under conditions of incomplete solvent relaxation, the half-width of the emission peak is markedly increased (Prendergast et al., 1983). This was also the case for the OSCP–acrylodan adduct in aqueous buffer; the half-width of its emission peak (4750 cm^{-1}) was in fact considerably wider than that of mercaptoethanol–acrylodan in aqueous

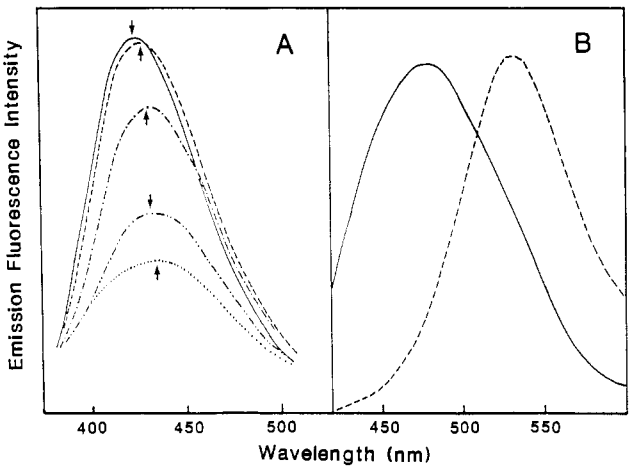

FIGURE 3: Effect of urea on the emission spectrum of OSCP–Mal-ANS. Panel A: OSCP–Mal-ANS (7.8 μg) was solubilized in 3 mL of standard medium in the presence of increasing concentrations of urea. Excitation was set at 322 nm. The λ_{max} values for the emission peaks designated by arrows were 422 nm for OSCP–Mal-ANS control (—) and 429, 432, 433, and 437 nm for OSCP–Mal-ANS in urea at concentrations of 3 M (- - -), 5 M (–·–), 6.6 M (–··–), and 10 M urea (···), respectively. Panel B: OSCP–acrylodan (4 μg) was solubilized either in standard medium (—) or in 6.6 M urea, 33 mM KCl, 7 mM Hepes, and 0.07% Tween 20, pH 7.4 (- - -). Excitation was set at 400 nm. The λ_{max} values for emission were 480 nm for OSCP–acrylodan in standard medium and 532 nm for OSCP–acrylodan in 6.6 M urea.

buffer (2800 cm^{-1}) or in ethanol (3000 cm^{-1}). Partial denaturation of OSCP by urea led to a decrease of the quantum yield of OSCP–Mal-ANS and a red shift of the emission peak for both OSCP–Mal-ANS (Figure 3A) and OSCP–acrylodan (Figure 3B), indicating that the probe bound to Cys 118 was more exposed to the aqueous medium. Consistent with this observation, denaturation of OSCP–Mal-pyrene by 6 M guanidinium chloride induced a 87% decrease of the pyrene fluorescence efficiency. Also noteworthy is the decrease of the half-width of the emission peak of OSCP–acrylodan from 4750 to 2980 cm^{-1} upon denaturation of OSCP by urea (Figure 3B). The latter half-width value is close to that of mercaptoethanol–acrylodan in aqueous medium, which makes it likely that mobility of the probe in denatured OSCP was greatly enhanced.

When F_1 was added to OSCP–acrylodan and OSCP–Mal-ANS, a red shift occurred; most probably the probe was exposed to a more polar medium upon binding of F_1 to OSCP (Table III). Moreover, in the case of OSCP–acrylodan supplemented with F_1, the half-width of the emission was lowered from 4750 to 4250 cm^{-1}, suggesting that in the F_1–OSCP complex the solvent molecules around Cys 118 relax faster than in OSCP alone. No significant shift was observed upon addition of F_1 to OSCP–Mal-coumarin, OSCP–Mal-pyrene, and OSCP–Mal-fluorescein (Table III), which results from the lower sensitivity of the emission maxima of these probes to solvent polarity (cf. Table II). On the other hand, the quantum yields of the OSCP–Mal-coumarin and OSCP–Mal-pyrene adducts were decreased upon addition of F_1. Emission decay analysis also showed a decrease of the lifetime of OSCP–Mal-pyrene from 88 to 72 ns upon addition of F_1. These last modifications of fluorescence parameters can be explained by a more complete exposure of the probe to the aqueous buffer and/or by the occurrence of additional static quenching processes in the presence of F_1 in the specific case of OSCP–Mal-coumarin.

Quenching Studies. Accessibility of OSCP-bound fluorescent probes was also analyzed by quenching studies with KI.

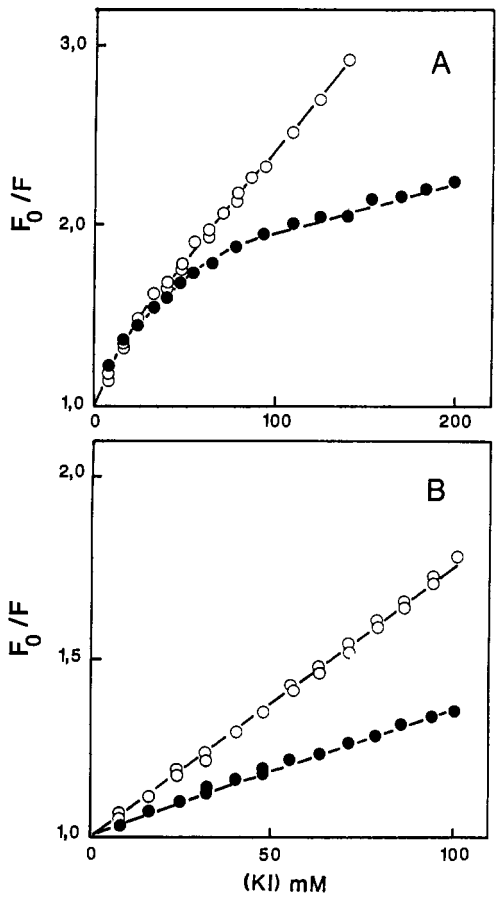

FIGURE 4: Quenching effect of KI on the OSCP–Mal-fluorescein and OSCP–Mal-pyrene adducts. Panel A: Quenching of OSCP–Mal-pyrene fluorescence. OSCP–Mal-pyrene (5.5 μg) was diluted either in standard medium (●) or in 6 M guanidinium chloride dissolved in standard medium (○). Then KI in 100 μM $Na_2S_2O_3$ was added at increasing concentrations, and fluorescence was measured (excitation set at 340 nm, emission measured with Baltzer filter K40). To compensate variations in the ionic strength, iodine was replaced by chloride. In guanidinium chloride, fluorescence of OSCP–Mal-pyrene was drastically decreased and a 10-min incubation was required to reach a stable fluorescence level before starting addition of KI. Panel B: Quenching of OSCP–Mal-fluorescein fluorescence. OSCP–Mal-fluorescein (2 μg) was diluted in standard medium either without (●) or with guanidinium chloride (○), as described in panel A.

As expected from the lifetime values, mercaptoethanol adducts of the different probes exhibited very different sensitivities to collisional quenching. For mercaptoethanol adducts of Mal-pyrene, Mal-fluorescein, acrylodan, Mal-ANS, and Mal-coumarin, the Stern–Volmer constants were equal to 80 M^{-1}, 9 M^{-1}, 3 M^{-1}, 0.17 M^{-1}, and 0.07 M^{-1}, respectively. The first three probes, which showed the highest sensitivity to KI, were further used for quenching studies (Figure 4). OSCP–Mal-fluorescein (Figure 4B) and OSCP–acrylodan (not shown) gave rectilinear Stern–Volmer plots, indicating a homogeneous population of bound probe molecules. The Stern–Volmer constants were 3 M^{-1} and 0.3 M^{-1}, respectively. Taking the lifetime values of the different adducts into account, the lower sensitivity of the OSCP adducts to KI is explained by assuming that the probes bound to OSCP are less exposed to the aqueous medium than those bound to mercaptoethanol. In OSCP, bound Mal-fluorescein appears to be more exposed to the medium than bound acrylodan. This might be the result of the polar nature of the ionized carboxylic group in fluorescein and thereby of its tendency to be extruded from the hydrophobic pocket surrounding Cys 118.

When compared to the mercaptoethanol adduct, OSCP–Mal-pyrene showed also a lower sensitivity to KI. The Stern–Volmer plots were curvilinear (Figure 4A), suggesting a heterogeneous population of bound Mal-pyrene which could be related to a heterogenous labeling of OSCP by Mal-pyrene; however, this possibility was ruled out by the finding that the decay curve for the lifetime was monoexponential and that Mal-pyrene was attached to a single peptide in the tryptic digest of labeled OSCP (see Figure 1B). An alternative explanation is the asymmetric nature of the Mal-pyrene molecule with two possible orientations of the bound Mal-pyrene with respect to the presumed hydrophobic pocket containing Cys 118. To ascertain that the decreased sensitivity of OSCP-bound probes to high quencher concentrations was not related to a trivial decrease of the rate of diffusion of the bound probe, a fluorescence quenching study at different concentrations of KI was performed with OSCP–Mal-pyrene and OSCP–Mal-fluorescein, after denaturation of OSCP in guanidinium chloride (panels A and B of Figure 4). In both cases, denaturation of OSCP made the bound probe more accessible to the quencher. The Stern–Volmer plots relative to denatured OSCP–Mal-fluorescein were strictly rectilinear like those of native OSCP–Mal-fluorescein (Figure 4B). The Stern–Volmer plots in the case of denatured OSCP–Mal-pyrene were virtually rectilinear, in contrast to the curvilinear plots of native OSCP–Mal-pyrene (Figure 4A). In brief, upon exposure to the aqueous solvent, the Mal-pyrene bound to denatured OSCP behaves with respect to the quencher KI as if it belongs to a homogeneous population of probe molecules, equally accessible to the quencher.

Addition of either F_1 or AUA submitochondrial particles (as a source of F_o) to OSCP–Mal-fluorescein and OSCP–Mal-pyrene had no noticeable effect on the accessibility of the bound probe to KI.

Polarization Studies. To explore the hydrodynamic properties of OSCP and the OSCP–F_1 complex, fluorescence polarization studies of the fluorescent derivatives of OSCP appeared to be a suitable approach. However, a choice had to be made among the available fluorescent probes used to label OSCP, based in particular on the value of their lifetime. For example, Mal-ANS, Mal-fluorescein, Mal-coumarin, and acrylodan bound to OSCP have short lifetimes (Table III), and consequently the predicted changes of polarization as a function of the solvent viscosity are not large enough for accurate calculation of molecular volumes. Indeed, the Perrin plots (cf. Materials and Methods) derived from polarization measurements performed with OSCP–Mal-ANS and OSCP–Mal-coumarin were characterized by slopes of very low value (not shown). In contrast, OSCP–Mal-pyrene exhibited a relatively long lifetime (Table III), and as expected, the corresponding slope of the Perrin plots had a measurable value (Figure 5). The derived molecular volume for OSCP–Mal-pyrene was 63 000 cm^3/mol. From the amino acid composition, a specific volume for OSCP of 0.755 cm^3/g (Cohn & Edsall, 1943) and a maximal hydration of 0.4 g of H_2O/g of protein (Kunts, 1971) could be calculated; thus the hydrated volume of OSCP could not exceed 25 000 cm^3/mol. The large difference between the predicted and experimental values of the volume of OSCP might be explained either by an aggregation phenomenon or by the asymmetrical shape of OSCP (Dupuis et al., 1983b). Aggregation was unlikely on the basis of the following lines of evidence. (1) Neutron scattering studies have shown that OSCP in aqueous solutions is monomeric and can be approximated to a prolate ellipsoid of axial ratio 3/1/1 (Dupuis et al., 1983b). (2) In gel filtration experiments with Superose 12, OSCP and OSCP–Mal-pyrene behaved as if they were in the monomeric state. It can

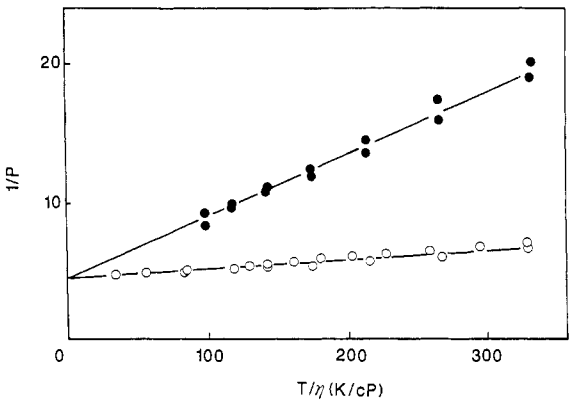

FIGURE 5: Perrin plot of the steady-state polarization of OSCP–Mal-pyrene fluorescence. OSCP–Mal-pyrene (15 μg) was incubated in standard medium either alone (○) or in the presence of 800 μg of F_1 (●). The fluorescence steady-state polarization (P) was measured as described under Materials and Methods. The viscosity η in centipoise (cP) of the medium was varied by addition of glycerol (Dean, 1976). The correlation time was calculated from the ratio of the slope of plots to $(1/P_0 - 1/3)$, where P_0 is the extrapolated value to $T/\eta = 0$. The absolute temperature T was 298 K.

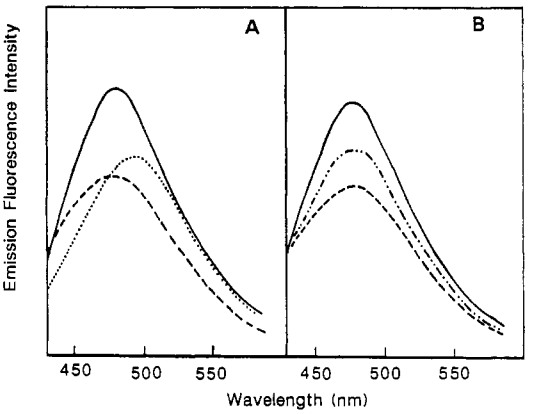

FIGURE 6: Effect of F_1 and AUA particles on the fluorescence emission spectrum of OSCP–acrylodan. To 2.5 mL of standard medium were added in the following order: (A) 2 μg of OSCP–acrylodan (---), 67 μg of F_1 (···), and finally 0.47 mg of AUA particles (—); (B) 2 μg OSCP–acrylodan (---), 0.47 mg of AUA particles (–··–), and finally 67 μg of F_1 (—). After each addition followed by a 10-min incubation at 20 °C, emission spectra were recorded. Excitation was set at 400 nm.

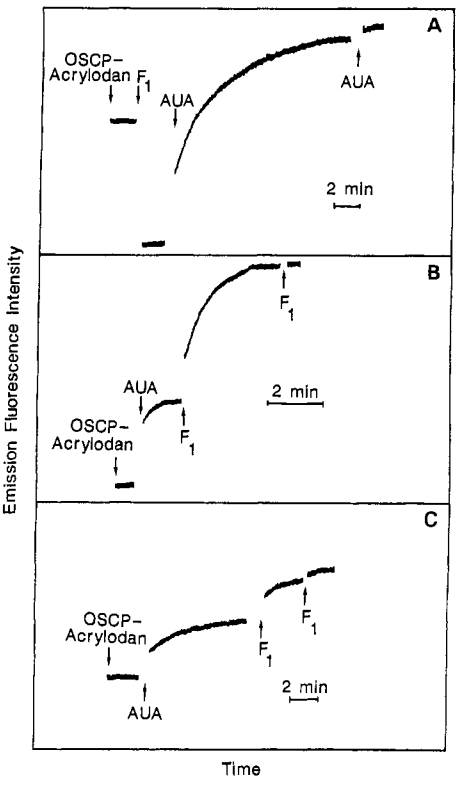

FIGURE 7: Kinetics of binding of OSCP–acrylodan to the F_1 and F_o sectors of the ATPase complex, monitored by fluorescence changes of the OSCP–acrylodan adduct. To 2.5 mL of a buffer medium consisting of standard medium supplemented with 1 mM $MgCl_2$ were added in the following order: (A) 2 μg of OSCP–acrylodan, 100 μg of F_1, and 0.47 mg of AUA particles (twice); (B) 2 μg of OSCP–acrylodan, 0.47 mg of AUA, and 100 μg of F_1 (twice); (C) 2 μg of OSCP–acrylodan, 0.47 mg of AUA, and 100 μg of F_1 (twice). Emission was measured at 450 nm for experiments A and C and at 490 nm for experiment B, with excitation wavelength set at 400 nm.

therefore be concluded that the apparent discrepancy between the experimental and predicted values of OSCP–Mal-pyrene is inherent in the asymmetrical shape of OSCP.

A polarization fluorescence study has also been carried out with F_1–OSCP–Mal-pyrene. From the Perrin plots, an apparent specific volume of 355 000 cm^3/mol was calculated for this complex. Taking 392 000 Da as the molecular mass of F_1–OSCP–Mal-pyrene and 0.735 cm^3/g as the specific volume, the volume of the F_1–OSCP–Mal-pyrene complex was found to be close to 300 000 cm^3/mol. Assuming the same degree of hydration for mitochondrial F_1 as for *Escherichia coli* F_1 (Paradies & Schmidt, 1979), i.e., 0.6 g of H_2O/g of protein, a volume of 520 000 cm^3/mol was derived for F_1–OSCP. The difference between the value of the F_1–OSCP complex deduced from the fluorescence data, i.e., 355 000 cm^3/mol, and the predicted value derived from the amino acid composition, i.e., 520 000 cm^3/mol, probably resulted from some relative mobility of OSCP in the OSCP–F_1 complex. It must be pointed out that no significant amount of free OSCP is expected to be present, as OSCP binds to F_1 with high affinity (Dupuis et al., 1985a; Dupuis & Vignais, 1987), and that there was a 3-fold molar excess of F_1 with respect to OSCP in the present experiment.

Conformational Changes in the OSCP–F_1 and OSCP–F_1–F_o Complexes As Probed by Acrylodan. To detect conformational changes at the level of Cys 118 of OSCP, depending on interactions of OSCP with F_1 and F_o, reconstitution experiments were performed with OSCP–acrylodan, because of the high fluorescence sensitivity of bound acrylodan.

The OSCP–acrylodan adduct had a maximal emission at 480 nm. Upon binding of F_1, the λ_{max} was shifted to 495 nm (Figure 6). Further binding to the F_o sector present in AUA particles resulted in a blue shift, so that the λ_{max} of the new peak was virtually the same as that of OSCP–acrylodan. This blue shift was probably minimized by the turbidity of the AUA particles preparation. No significant fluorescence shift was observed when F_o was added first to OSCP–acrylodan, and also when F_1 was further added, resulting in an F_1–F_o–OSCP complex.

The kinetics of the fluorescence changes was followed in the case of addition of F_1 and F_o to OSCP–acrylodan, with the excitation light set at 400 nm and the emission light set at 450 nm (Figure 7A,C) or 490 nm (Figure 7B). Addition of F_1 leading to the formation of the F_1–OSCP–acrylodan complex resulted in a fast decrease of the fluorescence intensity, which could not be kinetically resolved; the further addition of AUA particles leading to the formation of the F_1–F_o–OSCP–acrylodan complex initiated a slow enhancement of fluorescence, which took more than 10 min to achieve completion. On the other hand, addition of AUA particles to OSCP–acrylodan to form the F_o–OSCP–acrylodan complex resulted in a slow increase of fluorescence which attained a plateau in

about 4 min; a further addition of F_1 yielding the F_1–F_o–OSCP–acrylodan complex induced again a slow fluorescence rise, which reached completion in about 10 min.

Recently, Penefsky (1985) reported that addition of oligomycin or dicyclohexylcarbodiimide (DCCD), two ligands of the F_o sector, to submitochondrial particles resulted in conformational changes in the F_1 sector of the ATPase complex. A propagated change of conformation from F_o to F_1 was postulated. Possible conformational changes induced at the level of OSCP by the binding of oligomycin or DCCD to the F_o sector of AUA particles were explored, by using a reconstituted system made of F_1, AUA particles, and OSCP–acrylodan. No significant fluorescence change was detected under conditions of full inhibition by oligomycin or DCCD. Either there was no change of conformation of OSCP upon binding of oligomycin to F_o or, if a change of conformation occurred, it would be experienced by a region different from the area around the Cys 118 residue of OSCP.

Discussion

The present study on fluorescent derivatives of OSCP stems from the finding (Dupuis et al., 1985) that modification of the only cysteinyl residue of OSCP, Cys 118, does not modify the biological activity of this protein. Such probes are of high potential interest to study the dynamics of interactions of OSCP with the F_1 and F_o sectors in an attempt to elucidate the precise role of OSCP in the ATPase complex. To avoid artifacts inherent in the size or polarity of a given probe and in the specific interactions of this probe with the medium, a number of fluorescent probes have been used to label OSCP, and their fluorescence parameters in their bound form have been carefully assessed and compared. These probes were acrylodan and several maleimide derivatives, namely, Mal-ANS, Mal-pyrene, Mal-coumarin, and Mal-fluorescein.

Methods for separation of the fluorescent derivatives of OSCP have been improved, and the specific binding of the fluorescent probes to Cys 118 of OSCP has been demonstrated. The fluorescent derivatives of OSCP have been separated from the free probes by centrifugation–filtration on Sephadex G-50. This method proved to be more convenient and more rapid than that based on ammonium sulfate precipitation (Dupuis et al., 1985). It avoided dialysis, which is not appropriate to free proteins from hydrophobic reagents. As checked by thin-layer chromatography, no adsorbed probe was present in the isolated OSCP derivatives. Specific binding of the fluorescent probes to Cys 118 was checked by examination of the labeled peptide fragments obtained by tryptic digestion of labeled OSCP (Figure 1). A single fragment was found to be labeled by DTNB. The same fragment was labeled by the different fluorescent probes used in the present study. Only in the case of Mal-ANS was additional binding of the probe evidenced (not exceeding 30% of the total binding). Heterogeneous labeling of OSCP–Mal-ANS was consistent with the biexponential decay curve, giving two values of lifetime for OSCP–Mal-ANS (Table III).

With the different OSCP fluorescent derivatives, we have devised experiments to answer the two following questions: (1) What are the characteristics of the OSCP structure in the vicinity of Cys 118, in terms of accessibility, flexibility and polarity? (2) Is the Cys 118 neighborhood influenced by interaction of OSCP with the F_1 and/or F_o sectors of the ATPase complex?

Structural Features of the Peptide Chain of OSCP in the Vicinity of Cys 118. The fact that the emission peaks of the OSCP–acrylodan, OSCP–Mal-coumarin, and OSCP–Mal-ANS are blue-shifted with respect to the peaks of the corresponding mercaptoethanol derivatives in aqueous buffer indicated that the fluorophores attached to Cys 118 in OSCP were sequestered in a hydrophobic pocket. When compared to the mercaptoethanol derivatives in ethanol or acetonitrile, the emission maxima of the OSCP derivatives were relatively close, suggesting that the hydrophobic pocket in which Cys 118 is located has a polarizability similar to that of ethanol and acetonitrile. These conclusions are consistent with quenching data obtained with KI, showing that the fluorophore attached to Cys 118 was shielded from the aqueous buffer. They are also consistent with the fact that the quantum yield and lifetime values of the OSCP fluorescent derivatives are generally higher than those of the corresponding mercaptoethanol derivatives in aqueous medium.

Among the different fluorescent probes tested, acrylodan proved to be particularly useful to study hydrophobic pockets because of its extreme sensitivity to solvent polarity (Prendergast et al., 1983), a property shared by prodan, a closely related probe (Weber & Farris, 1979). As reported in the present work, the half-width of the OSCP–acrylodan emission peak, 4750 cm^{-1}, largely exceeded that of the corresponding mercaptoethanol adduct in water, 2800 cm^{-1}, indicating that the solvent molecules surrounding the excited fluorophore bound to Cys 118 of OSCP exhibited a long relaxation time, compared to the lifetime of the excited fluorophore in the conjugated OSCP. The incomplete relaxation of the environment around acrylodan bound to OSCP might be explained by lack of motion of the protein lattice surrounding Cys 118, which is consistent with the prediction based on the hydrophilicity profile and the secondary structure of beef heart OSCP (Ovchinnikov et al., 1985) that Cys 118 is at the boundary of a hydrophobic β sheet. Consistent with this interpretation was the finding that denaturation by urea induced a considerable decrease of the half-width of the emission peak of acrylodan–OSCP from 4750 to 2950 cm^{-1}.

Changes of the Fluorescence Properties of the Fluorophore Attached to Cys 118 in OSCP upon Binding of F_1 and F_o to OSCP. Fluorescence changes initiated by binding of F_1 to OSCP–fluorescent probe adducts can be explained by the exposure of the Cys 118 bound fluorophore to a more hydrophilic environment. These fluorescence changes were as follows. First, upon addition of F_1, the fluorescence peaks of the acrylodan and Mal-ANS derivatives of OSCP were red-shifted; second, the half-width of the emission peaks for the acrylodan derivative of OSCP became more narrow; third, the lifetime of the OSCP–Mal-pyrene adduct decreased from 88 to 72 ns; and fourth, the quantum yields for the OSCP–Mal-ANS, OSCP–Mal-coumarin, and OSCP–Mal-pyrene adducts were decreased.

Polarization data for OSCP–Mal-pyrene are consistent with the asymmetrical shape of OSCP (Dupuis et al., 1983b). The calculated molecular volume of the OSCP–Mal-pyrene adduct combined to F_1 was found to be lower than the molecular volume deduced from the amino acid composition. Probably, the OSCP–Mal-pyrene adduct exhibits some rotational freedom when combined with F_1.

Because of scattering artifacts related to the turbidity of AUA particles, it was not possible to extend to the ternary F_o–F_1–OSCP complex the study of fluorescent parameters undertaken with isolated OSCP or F_1-bound OSCP. We only explored the changes in the fluorescence intensity and wavelength maxima that followed the addition of the OSCP–acrylodan adduct to F_1 or to F_o or to both of them. Fluorescence changes in the emitted light depending on addition of F_1 indicated a fast reaction (achieved presumably

in much less than 1 s) between OSCP and F_1. In contrast, binding of OSCP to F_o (in AUA particles) required several minutes to achieve completion. Similarly, binding of F_o to OSCP–F_1 or binding of F_1 to OSCP–F_o were also slow reactions. These results add more credence to the postulate that OSCP primarily reacts with F_1 and induces a change of conformation of F_1 that favors its interaction with F_o (Dupuis & Vignais, 1987). The function of OSCP in the mitochondrial F_1–F_o complex ressembles that of the δ subunit in the bacterial ATPase complex. Indeed, whereas δ poorly binds to δ-depleted bacterial membranes, it combines with δ-depleted F_1, and the resulting F_1 binds efficiently to the membrane-bound F_o (Sternweiss & Smith, 1977). The behavior of the ϵ subunit in the chloroplast F_1–F_o complex has also some analogy with that of OSCP in the mitochondrial complex (Richter et al., 1984, 1985).

In experiments carried out with OSCP–acrylodan, it was found that the red shift of the emission peak that occurred when F_1 bound to OSCP–acrylodan was reversed upon addition of AUA particles. A likely explanation is that Cys 118 in OSCP which had become exposed to the aqueous medium upon binding of F_1 was shielded again upon binding of F_o and formation of the ternary complex F_o–F_1–OSCP.

ACKNOWLEDGMENTS

We thank Prof. G. Laustriat and Prof. D. Gêrard (University of Strasbourg) and Drs. J. Garin, J.-P. Issartel, and J. Lunardi (University of Grenoble) for their interest in this work and helpful discussions and R. Cêsarini and J. Bournet for secretarial assistance.

REFERENCES

Adams, M. J., Highfield, J. G., & Kirkbright, G. F. (1977) *Anal. Chem. 49*, 1850–1852.

Bradford, M. M. (1976) *Anal. Biochem. 72*, 248–254.

Chou, P. Y., & Fasman, G. D. (1974) *Biochemistry 13*, 211–221.

Cohn, E. J., & Edsall, J. T. (1943) in *Protein, Amino Acids and Peptides as Ions and Dipolar Ions* (Cohn, E. J., & Edsall, J. S., Eds.) pp 370–380, Rheinhold, New York.

Dean, J. A. (1973) in *Lange's Handbook of Biochemistry* (Dean, J. A., Ed.) 11th ed., pp 10–288, McGraw-Hill, New York.

Dupuis, A., & Vignais, P. V. (1985) *Biochem. Biophys. Res. Commun. 129*, 819–825.

Dupuis, A., & Vignais, P. V. (1987) *Biochemistry 26*, 410–418.

Dupuis, A., Satre, M., & Vignais, P. V. (1983a) *FEBS Lett. 156*, 99–102.

Dupuis, A., Zaccaï, G., & Satre, M. (1983b) *Biochemistry 22*, 5951–5956.

Dupuis, A., Issartel, J.-P., Lunardi, J., Satre M., & Vignais, P. V. (1985a) *Biochemistry 24*, 728–733.

Dupuis, A., Issartel, J. P., Lunardi, A., Satre, M., & Vignais, P. V. (1985b) in *Achievements and Perspectives of Mitochondrial Research* (Quagliariello, E., et al., Eds.) Vol. I, pp 237–246, Elsevier, New York.

Dupuis, A., Duszynski, J., & Vignais, P. V. (1987) *Biochem. Biophys. Res. Commun. 142*, 31–37.

Ernster, L., Hundal, T., & Sandri, G. (1986) *Methods Enzymol. 126*, 428–433.

Gêrard, D., Laustriat, G., & Lami, H. (1972) *Biochim. Biophys. Acta 263*, 482–495.

Grinwald, A. (1976) *Anal. Biochem. 75*, 260–280.

Grinwald, A., & Steinberg, I. Z. (1974) *Anal. Biochem. 59*, 583–598.

Gupte, S. S., & Lane, L. K. (1979) *J. Biol. Chem. 254*, 10362–10367.

Gupte, S. S., & Lane, L. K. (1983) *J. Biol. Chem. 258*, 5005–5012.

Knowles, A. F., & Penefsky, H. S. (1972) *J. Biol. Chem. 247*, 6617–6623.

Kuntz, I. D. (1971) *J. Am. Chem. Soc. 93*, 514–516.

Lux, B., & Gêrard, D. (1981) *J. Biol. Chem. 256*, 1767–1771.

Nicholls, D. G. (1982) in *Bioenergetics. An Introduction to the Chemiosmotic Theory*, pp 151–164, Academic, London and New York.

Ovchinnikov, Y. A., Modyanov, N. N., Grinkevich, V. A., Aldanova, N. A., Trubetskaya, O. E., Nazimov, I. V., Hundal, T., & Ernster, L. (1984) *FEBS Lett. 166*, 19–22.

Ovchinnikov, Y. A., Modyanov, N. N., Grinkevich, V. A., Belogradov, G. I. Hundal, T., Norling, B., Sandri, G., Wojtczak, L., & Ernster, L. (1985) in *Achievements and Perspectives of Mitochondrial Research* (Quagliariello E., et al., Eds.) Vol. I, pp 223–236, Elsevier, New York.

Paradies, H. H., & Schmidt, U. D. (1979) *J. Biol. Chem. 254*, 5257–5263.

Parker, C. A., & Rees, W. T. (1960) *Anal. Chem. 85*, 587–600.

Penefsky, H. S. (1985) *Proc. Natl. Acad. Sci. U.S.A. 82*, 1589–1593.

Penin, F., Delêage, G., Godinot, C., & Gautheron, D. C. (1986) *Biochim. Biophys. Acta 852*, 55–67.

Prendergast, F. G., Meyer, M., Carlson, G. L., Iida, S., & Potter, J. D. (1983) *J. Biol. Chem. 258*, 7541–7544.

Richter, M. L., Patrie, W. J., & McCarty, R. E. (1984) *J. Biol. Chem. 259*, 7371–7373.

Richter, M. L., Snyder, B., McCarty, R. E., & Hammes, G. G. (1985) *Biochemistry 24*, 5755–5763.

Senior, A. E. (1979) *Methods Enzymol. 55*, 391–397.

Smith, A. L. (1967) *Methods Enzymol. 10*, 81–86.

Sternweiss, P. C., & Smith, J. B. (1977) *Biochemistry 16*, 4020–4025.

Weber, G., & Farris, F. J. (1979) *Biochemistry 18*, 3075–3078.

Zak, B., & Cohen, J. (1961) *Clin. Chim. Acta 6*, 665–670.